Reactions of Nitriles at Semiconductor Surfaces

Collin Mui, Michael A. Filler, and Stacey F. Bent

Department of Chemical Engineering, Stanford University, Stanford, California 94305-5025

Charles B. Musgrave*

Departments of Chemical Engineering and Materials Science and Engineering, Stanford University, Stanford, California 94305-5025

Received: April 2, 2003; In Final Form: June 24, 2003

Motivated by the recent interest in using nitriles for organic modification of semiconductor surfaces, we have used density functional theory and cluster models to study the reactions of nitriles on semiconductor surfaces. In particular, we have calculated the energetics for the surface reactions of acetonitrile, 2-propenenitrile, and 3-butenenitrile on the Si(100)-2 × 1 and Ge(100)-2 × 1 surfaces. For acetonitrile, our calculations predict that although it forms multiple products on the Si(100)-2 × 1 surface, the molecule does not react on the Ge(100)-2 × 1 surface. For 2-propenenitrile, the calculations show that whereas the C═C [2 + 2] cycloaddition product is thermodynamically most stable, formation of the hetero-[4 + 2] product is kinetically favored. We also have investigated the possibility of surface-catalyzed isomerization of 3-butenenitrile to 2-butenenitrile on the Si(100)-2 × 1 and Ge(100)-2 × 1 surface. We find that there are multiple surface-catalyzed isomerization pathways on the Si(100)-2 × 1 and Ge(100)-2 × 1 surfaces. However, our calculated kinetics predicts that the amount of 2-butenenitrile formed by surface-catalyzed isomerization is small.

Introduction

The unique structural and electronic properties of group-IV semiconductor surfaces have motivated intense research interest in their chemical reactivity toward organic molecules over the past several years.[1−4] This is because the ability to controllably attach multifunctional compounds to semiconductor surfaces is a crucial step toward the creation of hybrid organic−semiconductor devices, which may lead to applications ranging from molecular electronics to biocompatible device implantation. Therefore, recent research efforts in this area are focused on exploring chemical strategies to attach organic functional groups onto semiconductor surfaces, as well as comparing the reactivities of organic functional groups on different semiconductor surfaces.

Recently, nitrile compounds have been proposed as promising candidates for molecular layer growth of organics on semiconductor surfaces.[5−9] Specifically, it has been shown that the nitrile functional group does not react with the Ge(100)-2 × 1 surface.[7] This implies that one could attach a nitrile-containing multifunctional compound onto the Ge(100)-2 × 1 surface selectively, with the nitrile group intact for second layer attachment of other functional groups. Therefore, we investigate the chemistry of nitriles on the Si(100)-2 × 1 and Ge(100)-2 × 1 surfaces to develop an atomic level understanding of the reactivity of the nitrile functional group on semiconductor surfaces. We have used density functional theory (DFT) to calculate the reaction mechanisms, energetics, and associated kinetics of acetonitrile ($CH_3-C\equiv N$), 2-propenenitrile ($CH_2=CH-C\equiv N$), and 3-butenenitrile ($CH_2=CH-CH_2-C\equiv N$) on the Si(100)-2 × 1 and Ge(100)-2 × 1 surfaces (Figure 1). In this paper, we discuss the competition and selectivity of reactions with multifunctional nitrile compounds, as well as their similarity and differences on the Si(100)-2 × 1 and Ge(100)-2 × 1 surfaces. A complementary study using multiple internal reflection Fourier transform infrared (MIR-FTIR) spectroscopy has been published separately.[7]

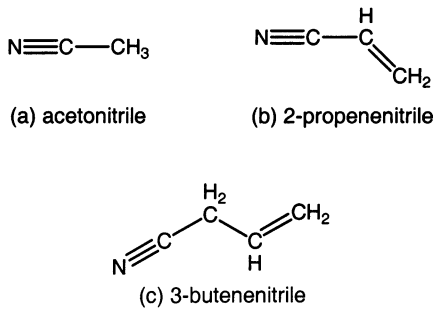

Figure 1. Nitrile compounds investigated in this work. (a) Acetonitrile, $CH_3-C\equiv N$; (b) 2-propenenitrile, $CH_2=CH-C\equiv N$; and (c) 3-butenenitrile, $CH_2=CH-CH_2-C\equiv N$.

Acetonitrile ($CH_3-C\equiv N$) is the simplest organic nitrile. The nitrile functional group consists of a nitrogen lone pair and a carbon−nitrogen triple bond, both of which can interact with the surface. While the nitrogen lone pair can donate its electrons to form a dative bond with the electrophilic down atoms of the Si(100)-2 × 1 and Ge(100)-2 × 1 surface dimers (Figure 2a), the orthogonal π-orbitals of the C≡N functional group can undergo [2 + 2] cycloaddition with the π-bond of the surface dimers (Figure 2b). In addition, acetonitrile can react with the Si(100)-2 × 1 and Ge(100)-2 × 1 surfaces via α-hydride elimination analogous to the "ene" reaction in organic chemistry, which results in the formation of a linear ketenimine species and an adsorbed hydrogen on the surface (Figure 2c). In a recent report by Tao et al. using temperature-programmed desorption

* Corresponding author. E-mail: charles@chemeng.stanford.edu.

10.1021/jp034864t CCC: $25.00 © 2003 American Chemical Society
Published on Web 10/14/2003

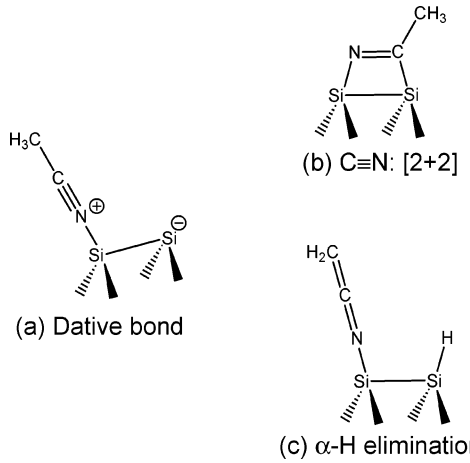

Figure 2. Possible surface reaction products of acetonitrile on the Si(100)-2 × 1 and Ge(100)-2 × 1 surfaces. (a) Dative bond formation; (b) C≡N [2 + 2] cycloaddition; and (c) α-hydride elimination, or ene reaction. Possible reaction products on the Ge(100)-2 × 1 surface are the same and are not shown.

(TPD), X-ray photoelectron spectroscopy (XPS), and high-resolution electron energy loss spectroscopy (HREELS), it was proposed that acetonitrile reacts on the Si(100)-2 × 1 surface via C≡N [2 + 2] cycloaddition at 110 K, and the chemisorbed product desorbs molecularly, resulting in two desorption features at 400 and 467 K.[5] On the other hand, Bournel et al. using photoemission spectroscopy (PES) and near-edge X-ray absorption fine structure (NEXAFS) spectroscopy concluded that acetonitrile reacts on the Si(100)-2 × 1 surface at 300 K to form the C≡N [2 + 2] product, along with other C≡N-bearing and dissociated products.[10] On the Ge(100)-2 × 1 surface, experiments in our laboratory using MIR-FTIR show that acetonitrile does not react at all at 300 K.[7]

2-Propenenitrile (CH_2═CH−C≡N) contains a C═C π-bond conjugated with the C≡N functional group. Similar to acetonitrile, 2-propenenitrile can undergo dative bond formation (Figure 3a), C≡N [2 + 2] cycloaddition (Figure 3b) and α-hydride elimination (Figure 3c) surface reactions. In addition, the conjugated C═C and C≡N π-system of 2-propenenitrile can react with the surface via the hetero-[4 + 2] cycloaddition reaction (Figure 3d), which is analogous to the Diels−Alder reaction. A C═C [2 + 2] cycloaddition of 2-propenenitrile on the surface is also possible (Figure 3e). Our calculations show that the dative-bonded state is a precursor to all the surface reaction products except the C═C [2 + 2] cycloaddition product, as summarized in Figure 3. It was proposed, on the basis of HREELS experiments, that 2-propenenitrile reacts selectively with the Si(100)-2 × 1 surface via C≡N [2 + 2] cycloaddition at 110 K.[5] However, a combined XPS and MIR-FTIR study by Schwartz et al. shows that although hetero-[4 + 2] cycloaddition is the major reaction pathway for 2-propenenitrile on the Si(100)-2 × 1 surface at 300 K, minor products containing C═C and C≡N functional groups, indicative of the C≡N [2 + 2] and C═C [2 + 2] cycloaddition reactions, respectively, were also observed.[11] These results are consistent with the recent PES and NEXAFS study by Bournel et al.[10] On the other hand, a recent theoretical study by Choi and Gordon shows that the reaction of 2-propenenitrile on the Si(100)-2 × 1 surface via hetero-[4 + 2] and C≡N [2 + 2] cycloaddition has low activation barriers of 3.3 and 4.0 kcal/mol, respectively, whereas reaction via C═C [2 + 2] cycloaddition requires a 16.7 kcal/mol activation barrier.[12] On the Ge(100)-2 × 1 surface, our experimental results show that the hetero-[4 + 2] reaction is the major reaction pathway.[7]

3-Butenenitrile (CH_2═CH−CH_2−C≡N) is a nonconjugated compound which contains a C≡N functional group and a C═C double bond, and is not expected to undergo hetero-[4 + 2] reaction due to the absence of conjugated π-bonds. However, the IR spectrum of 3-butenenitrile chemisorbed on the Si(100)-2 × 1 surface[11] at 300 K shows a C═C═N asymmetric

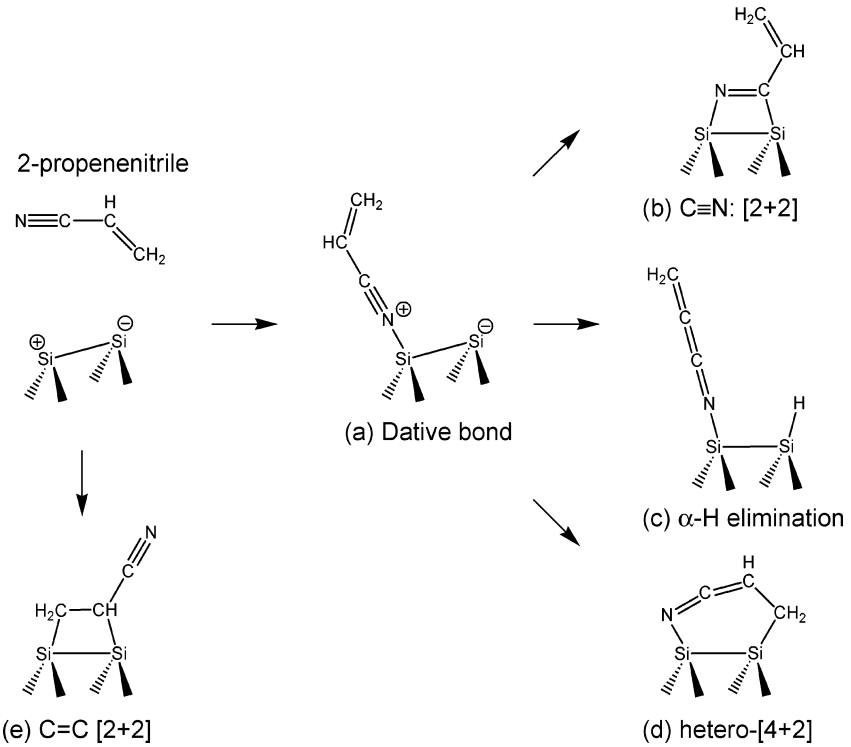

Figure 3. Possible surface reaction products of 2-propenenitrile on the Si(100)-2 × 1 and Ge(100)-2 × 1 surfaces. (a) Dative bond formation; (b) C≡N [2 + 2] cycloaddition; (c) α−hydride elimination, or ene reaction; and (d) hetero-[4 + 2] reaction to form a surface ketenimine product. Possible reaction products on the Ge(100)-2 × 1 surface are the same and are not shown.

stretching peak at 1982 cm^{-1}. Since the C═C═N asymmetric vibrational mode is a signature of the hetero-[4 + 2] product of a conjugated nitrile like 2-butenenitrile, Schwartz et al. proposed that the hetero-[4 + 2] product of 2-butenenitrile is one of the possible reaction products of 3-butenenitrile on the Si(100)-2 × 1 surface.[11] Similarly, the IR spectrum of 3-butenenitrile chemisorbed on the Ge(100)-2 × 1 surface[7] at 300 K shows a C═C═N asymmetric stretching peak at 1954 cm^{-1}. However, further IR experiments by Filler et al. have suggested that 3-butenenitrile can isomerize to 2-butenenitrile in the gas-handling system *before* reaction on the Ge(100)-2 × 1 surface.[7]

In this paper, we simulate and attempt to predict the chemistry of nitrile compounds on the Si(100)-2 × 1 and Ge(100)-2 × 1 surfaces using DFT. The reactivity of acetonitrile on the two surfaces is compared and the low kinetic stability of acetonitrile on the Ge(100)-2 × 1 surface is predicted. Kinetic competition between multiple reaction pathways of 2-propenenitrile on the Si(100)-2 × 1 surface, and the selectivity of the Ge(100)-2 × 1 surface toward the hetero-[4 + 2] product, are discussed. For 3-butenenitrile, several possible surface-catalyzed isomerization pathways of the nonconjugated nitrile to *cis*- and *trans*-2-butenenitrile, on both the Si(100)-2 × 1 and Ge(100)-2 × 1 surfaces, are presented in order to explore the possibility of isomerization reactions on semiconductor surfaces. In addition, the kinetics of the isomerization processes, as well as the relative amounts of products formed from surface-catalyzed isomerization, are discussed.

Computational Details

Our theoretical approach is based on density functional theory (DFT)[13,14] with the electronic structure expanded in atomic Gaussian basis functions. The Si_9H_{12} and $Ge_2Si_7H_{12}$ one-dimer clusters are used to model the Si(100)-2 × 1 and Ge(100)-2 × 1 surfaces, respectively (Figure 4a,b). The $Ge_2Si_7H_{12}$ cluster is constructed by replacing the dimer atoms on the Si_9H_{12} cluster with Ge atoms. The one-dimer cluster consists of two surface atoms representing the surface dimer, and seven atoms representing three layers of subsurface bulk atoms. The dangling bonds of the subsurface atoms are terminated by twelve hydrogen atoms in order to mimic the sp^3 hybridization of the silicon lattice. The Si_9H_{12} and $Ge_2Si_7H_{12}$ clusters have been used previously to model surface chemistry of organic compounds on the Si(100)-2 × 1 and Ge(100)-2 × 1 surfaces, respectively, and the results are consistent with experimental observations.[15,16] To study surface reactions involving two adjacent surface dimers along a dimer row, the $Si_{15}H_{16}$ and $Ge_4Si_{11}H_{16}$ two-dimer clusters are used to model the Si(100)-2 × 1 and Ge(100)-2 × 1 surfaces, respectively. The two-dimer clusters consist of 4 surface dimer atoms and 11 subsurface Si atoms arranged in four layers, as shown in Figure 4c,d.

We use the B3LYP/6-31G(d) level of theory[17,18] to determine the geometries of the critical points on the potential energy surface. Structures are fully optimized without geometrical constraints on the clusters, and symmetry restrictions are applied where appropriate. All minima and transition states are verified to have zero and one imaginary frequency, respectively. The imaginary normal modes of all the transition states are visually inspected to ensure that the transformations connect the corresponding reactant and product of each reaction. To improve the accuracy of the calculations, single-point energy calculations are then performed on the optimized structures at the B3LYP/6-311++G(2df,pd) level of theory. All energies reported are zero-point corrected. The electronic structure calculations in this work are performed using the *Gaussian 98* suite of programs.[19]

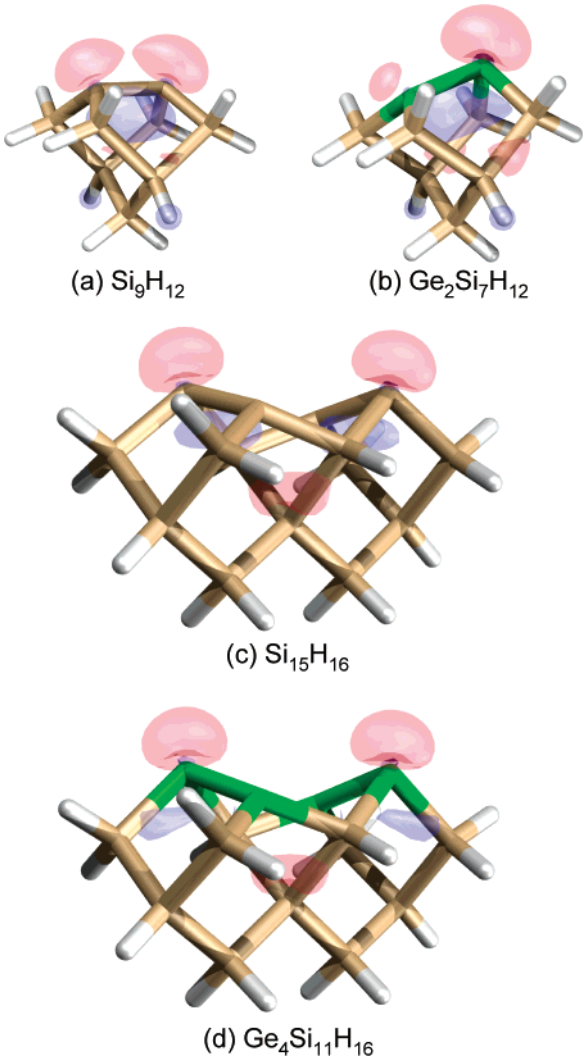

Figure 4. Cluster models for the Si(100)-2 × 1 and Ge(100)-2 × 1 surfaces. Highest occupied molecular orbital diagrams (HOMO) of the optimized structures are shown. (a) Si_9H_{12} one-dimer cluster; (b) $Ge_2Si_7H_{12}$ one-dimer cluster; (c) $Si_{15}H_{16}$ two-dimer cluster; and (d) $Ge_4Si_{11}H_{16}$ two-dimer cluster. Si atoms are in gold, Ge atoms are in green, and H atoms are in white.

Results and Discussion

Acetonitrile. We begin our discussion with the simplest organic nitrile, acetonitrile ($CH_3-C\equiv N$), in which the nitrile functionality is bonded only to a methyl group. The initial step of the acetonitrile surface reaction on the Si(100)-2 × 1 and Ge(100)-2 × 1 surfaces involves formation of a dative bond between the N lone pair of the C≡N group and the electrophilic down atom of the surface dimer (Figure 5). Dative bond formation of acetonitrile is exothermic on both the Si(100)-2 × 1 and Ge(100)-2 × 1 surfaces, with adsorption energies calculated to be 14.0 and 11.1 kcal/mol, respectively. Application of simple first order kinetic analysis with a typical preexponential factor[20] of 10^{13} sec^{-1} reveals that dative-bonded acetonitrile has a desorption half-life of 1 ms and 9 μs, respectively, on the Si(100)-2 × 1 and Ge(100)-2 × 1 surfaces at 300 K. This indicates that dative-bonded acetonitrile is not kinetically stable on either surface at 300 K, which means that the lifetime of dative-bonded acetonitrile is much shorter than the experimental time scale.

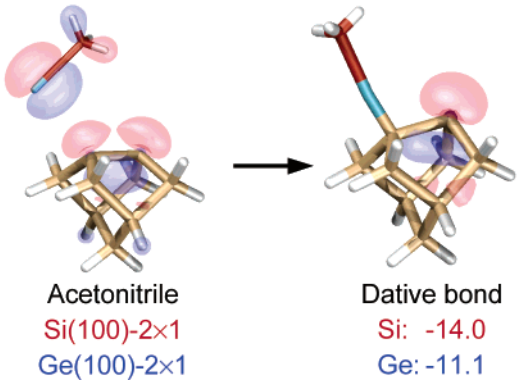

Figure 5. Reaction of acetonitrile on the Si(100)-2 × 1 and Ge(100)-2 × 1 surfaces via dative bond formation. Optimized structure on the Si_9H_{12} cluster is shown. Energies are in kcal/mol and are zero-point corrected. N atoms are in blue, C atoms are in red, and H atoms are in white.

Dative bond formation involves electron donation from the lone pair to the electrophilic down atom of the dimer on the Si(100)-2 × 1 and Ge(100)-2 × 1 surfaces. The interaction is analogous to a Lewis acid−base reaction. Therefore the strength of a surface dative bond is related to the acidity of the electrophilic dimer atom, as well as the basicity of the lone pair. Our calculations show that the adsorption energy for acetonitrile on the Ge−Ge dimer is slightly lower than that on the Si−Si dimer, and similar trends were observed for the initial adsorption of amines[21] and ketones.[22,16] This indicates that the down Si atom of the Si−Si dimer is slightly more electrophilic than the down atom of the Ge−Ge dimer. Interestingly, for both surfaces, initial adsorption of acetonitrile results in weaker surface dative bonds (11−14 kcal/mol) than does the adsorption of dimethylamine on the Si(100)-2 × 1 and Ge(100)-2 × 1 surfaces (24−25 kcal/mol).[21] Because the lone pairs of nitriles are *sp*-hybridized whereas those of amines are sp^3-hybridized, nitriles are generally weaker bases than amines,[23] and therefore they will form weaker dative bonds with the Si(100)-2 × 1 and Ge(100)-2 × 1 surfaces, consistent with our theoretical results.

The dative-bonded state of acetonitrile is a precursor to both C≡N [2 + 2] cycloaddition and α-hydride elimination reactions on the Si(100)-2 × 1 and Ge(100)-2 × 1 surfaces. The calculated reaction pathways at the Si(100)-2 × 1 and Ge(100)-2 × 1 surfaces are shown in Figure 6. We find that although α-H elimination of acetonitrile leads to more stable surface products, C≡N [2 + 2] cycloaddition has lower activation barriers on both the Si(100)-2 × 1 and Ge(100)-2 × 1 surfaces. Similar energetic trends are observed for competing C═O [2 + 2] and α-H elimination surface reactions of dative-bonded acetone on the Ge(100)-2 × 1 surface, where the ene reaction is thermodynamically favorable but kinetically unfavorable compared to the C═O [2 + 2] cycloaddition.[22]

When the reaction energetics of acetonitrile on the Si(100)-2 × 1 and Ge(100)-2 × 1 surface are compared, it is found that reactions on the Si(100)-2 × 1 surface have lower activation barriers and are more exothermic. The calculated energetics on the two surfaces are consistent with periodic trends of group-IV elements. In general, bond strength and lone-pair basicity decrease down a group. The stronger Si−H and Si−C bonds formed between acetonitrile and the Si(100)-2 × 1 surface together with the fact that the up Si atom of the Si−Si dimer is

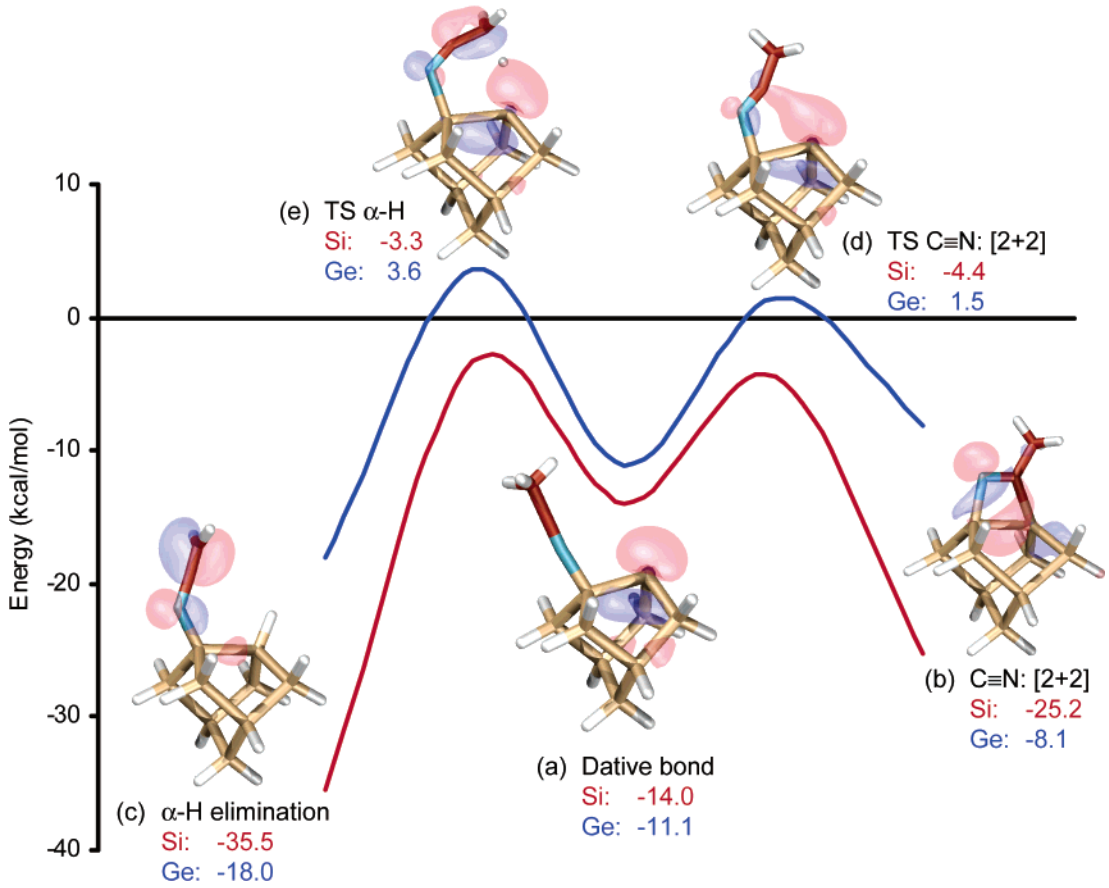

Figure 6. Reaction pathways of dative-bonded acetonitrile on the Si_9H_{12} cluster. The red and blue curves depict the reaction paths on the Si(100)-2 × 1 and Ge(100)-2 × 1 surfaces, respectively. Optimized HOMOs on the Si_9H_{12} cluster are shown. (a) Dative bond; (b) C≡N [2 + 2]; (c) α-hydride elimination; (d) transition state for C≡N [2 + 2]; and (e) transition state for α-hydride elimination.

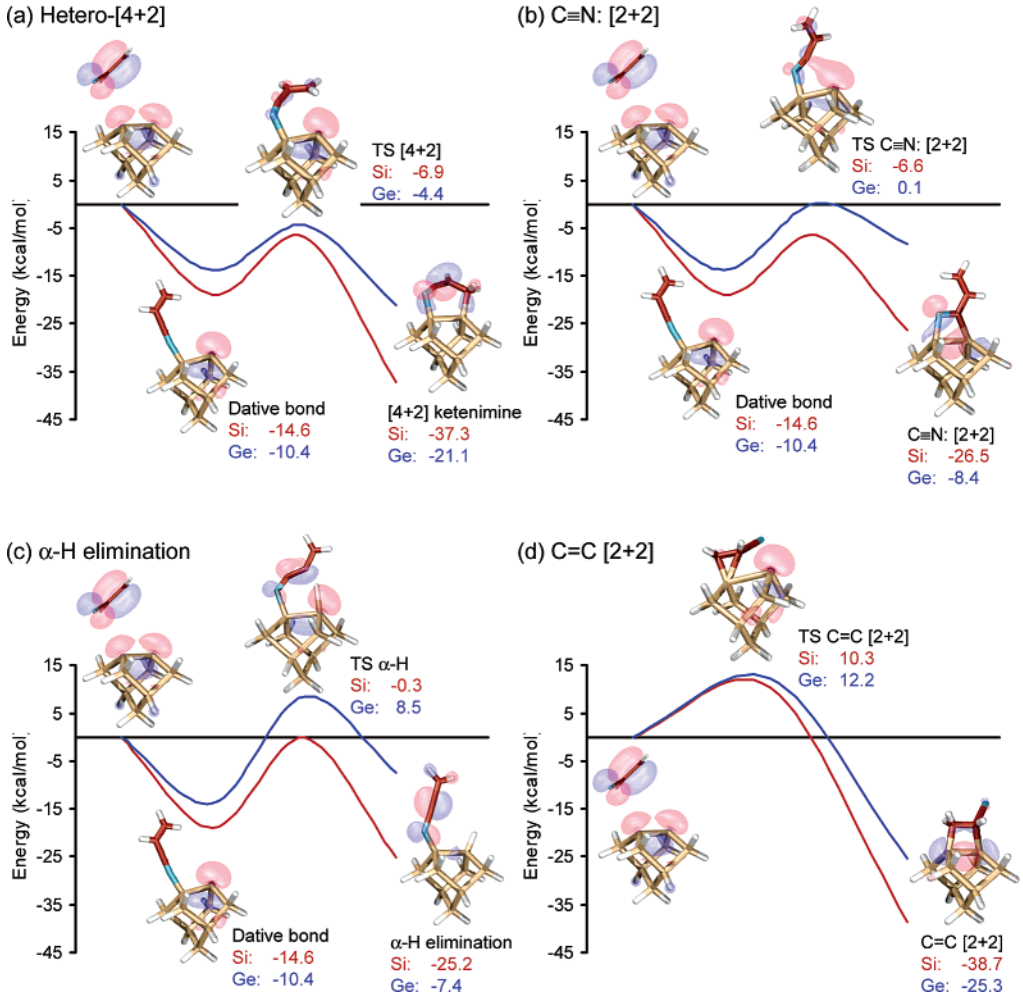

Figure 7. Reaction pathways of 2-propenenitrile on the Si(100)-2 × 1 and Ge(100)-2 × 1 surfaces, shown by the red and blue curves, respectively. Optimized HOMOs on the Si_9H_{12} cluster are shown. (a) Hetero-[4 + 2] cycloaddition or ketenimine formation; (b) C≡N [2 + 2] cycloaddition; (c) α-hydride elimination; and (d) C═C [2 + 2] cycloaddition.

more basic than the corresponding Ge atom of the Ge−Ge dimer result in higher reaction energies and lower activation barriers for the α-H elimination and C≡N [2 + 2] cycloaddition reactions on the Si(100)-2 × 1 surface compared to the reaction energies on the Ge(100)-2 × 1 surface. Similar periodic trends on bond strength and lone-pair basicity have been successfully applied to explain the chemistry of amines on group-IV semiconductor surfaces.[21]

The surface reaction energetics calculated by B3LYP-DFT are consistent with experimental observations. TPD and HREELS experiments at 110 K show that acetonitrile reacts on the Si(100)-2 × 1 surface selectively via C≡N [2 + 2] cycloaddition.[6] PES and NEXAFS experiments also identified the C≡N [2 + 2] product along with dissociated products on the Si(100)-2 × 1 surface at 300 K.[10] The calculated activation barrier for C≡N [2 + 2] cycloaddition is lower than that for the competing α-H elimination reaction, and hence C≡N [2 + 2] cycloaddition should be faster. Although the difference between the activation barriers for the two surface reactions is only 1.1 kcal/mol, the resulting branching ratio of the two pathways is 153 at 110 K if the surface reactions are irreversible. Therefore the population of the α-H elimination product is probably below the detection limit of HREELS. However, the branching ratio of the two reactions decreases to 6 at 300 K, and thus at 300 K kinetic competition between the two pathways, which should lead to the formation of some α-H elimination product on the Si(100)-2 × 1 surface. Although not explicitly discussed by Bournel et al.,[10] we believe that one of the many products seen on the Si(100)-2 × 1 surface at 300 K is the α-H elimination product. Although the agreement between our calculations and the experiments may be fortuitous due to the fact that the uncertainty of B3LYP-DFT is typically a few kcal/mol, this simple branching ratio analysis shows that the product distribution for competing reactions with similar activation barriers can be largely affected by surface temperature.

MIR-FTIR indicates that acetonitrile does not react on the Ge(100)-2 × 1 surface at 300 K.[7] Our calculations predict that the desorption half-lives of the dative-bonded precursor, C≡N [2 + 2] cycloaddition and α-H elimination products, with binding energies of 11.1, 8.1, and 18.0 kcal/mol, respectively, are all below 1 s at 300 K. Although all the surface reactions are exothermic on the Ge(100)-2 × 1 surface, none of the reaction products are kinetically stable on the surface with respect to reversible desorption at 300 K. Therefore, our calculations predict that no product from the reaction of acetonitrile with the Ge(100)-2 × 1 surface will be observed at 300 K, consistent with the experimental measurements.[7]

2-Propenenitrile. The conjugated π-system in 2-propenenitrile (CH_2═CH−C≡N) results in four reaction pathways at the Si(100)-2 × 1 and Ge(100)-2 × 1 surfaces (Figure 3). In addition to the C≡N [2 + 2] cycloaddition and α-hydride elimination reactions, 2-propenenitrile can also undergo a hetero-[4 + 2] cycloaddition reaction, which results in a six-membered surface ring ketenimine product, and C═C [2 + 2] cyclo-

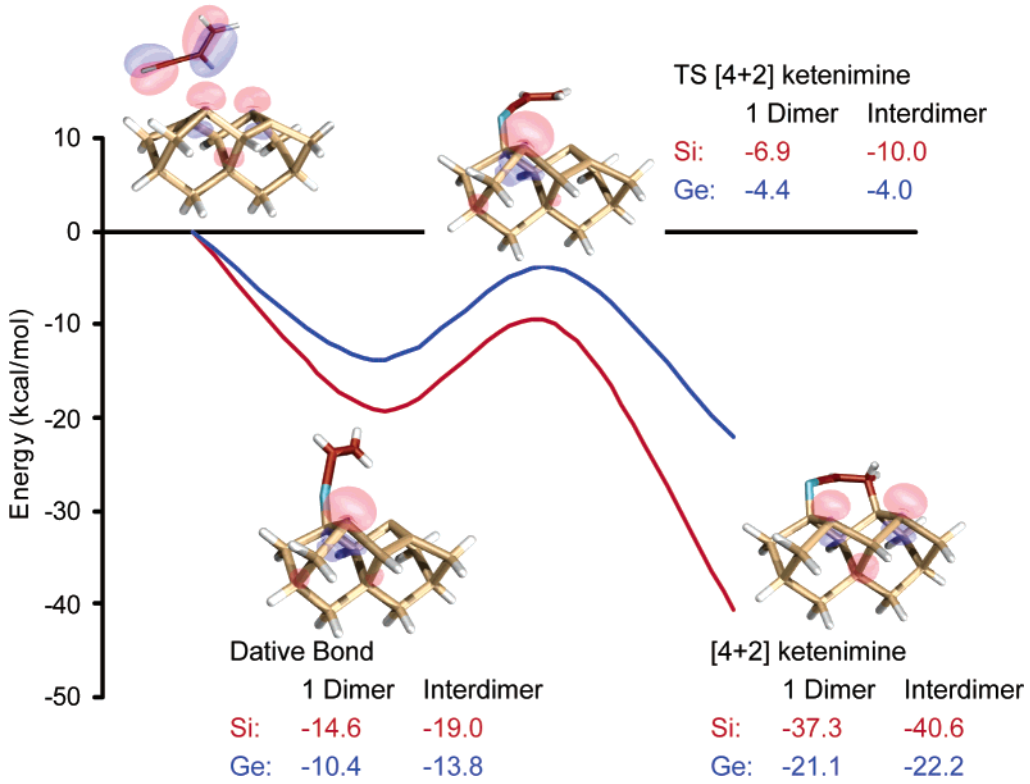

Figure 8. Interdimer [4 + 2] reaction paths of 2-propenenitrile on the $Si_{15}H_{16}$ and $Ge_4Si_{11}H_{16}$ clusters, shown by the red and blue curves, respectively. Optimized HOMOs on the $Si_{15}H_{16}$ cluster are shown. A surface ketenimine is formed across two adjacent dimers on the dimer row in each case. Energetics for the reaction on a single dimer are also shown for comparison.

addition, which results in a four-membered ring on the surface. Dative-bonded 2-propenenitrile is a precursor for all the reaction pathways except the C═C [2 + 2] cycloaddition reaction.

When the reaction pathways of 2-propenenitrile are compared (Figure 7), our calculations show that the C═C [2 + 2] cycloaddition reaction results in the most stable product, while the hetero-[4 + 2] reaction has the lowest activation barrier with respect to the energy of the reactants on both the Si(100)-2 × 1 and Ge(100)-2 × 1 surfaces. Kinetic analysis using a typical preexponential factor[20] for surface reactions (10^{13}) suggests that the reaction products with adsorption energies lower than 18 kcal/mol have desorption half-lives of less than 1 s, which is much shorter than the time scale of the experiment, and thus they will not be observed as stable products. Therefore, our calculations predict that whereas all reaction products should be stable on the Si(100)-2 × 1 surface at 300 K, only the hetero-[4 + 2] and C═C [2 + 2] products will be stable on the Ge(100)-2 × 1 surface at the same temperature.

Choi and Gordon have performed MRMP2 and CASSCF calculations for the reaction of 2-propenenitrile on the Si(100)-2 × 1 surface.[12] Their calculations predict that the adsorption energies for the hetero-[4 + 2], C≡N [2 + 2], and C═C [2 + 2] products are 20.6, 16.2, and 30.4 kcal/mol, respectively, while the activation barriers for the three surface reactions are 3.3, 4.0, and 16.7 kcal/mol, respectively. Their MRMP2 calculations predict that whereas the C═C [2 + 2] cycloaddition product is energetically the most favorable on the Si(100)-2 × 1 surface, the hetero-[4 + 2] reaction is kinetically the most favorable on the surface. Our calculations are consistent with Choi and Gordon's results, where we predict the same energetic trends for the reaction of 2-propenenitrile on the Si(100)-2 × 1 surface.

When the calculated energetics of the reaction pathways on the Si(100)-2 × 1 and Ge(100)-2 × 1 surfaces are compared, the results show that the reaction products are more stable energetically on the Si(100)-2 × 1 surface, and the activation barriers are generally lower. Similar to the discussion on acetonitrile surface reactions, stronger bonds formed on the Si−Si dimer and higher nucleophilicity of the up Si dimer atom are responsible for the higher reaction energies and lower activation barriers observed on the Si(100)-2 × 1 surface. An exception is the hetero-[4 + 2] reaction, for which the activation barrier measured from the dative-bonded state on the Si(100)-2 × 1 surface (7.7 kcal/mol) is higher than that on the Ge(100)-2 × 1 surface (6.0 kcal/mol). This exception can be explained by the difference in the bond lengths of the Si−Si (2.22 Å) and Ge−Ge dimers (2.33 Å), which results in different strain environments for the hetero-[4 + 2] transition states on the Si(100)-2 × 1 and Ge(100)-2 × 1 surfaces.

In addition to the higher activation barriers observed on the Ge(100)-2 × 1 surface, our calculations also show that the differences between the barriers for competing reactions are larger on the Ge(100)-2 × 1 surface. For example, the difference in the activation barriers between the hetero-[4 + 2] and the α-H elimination surface reactions is 6.6 kcal/mol on the Si(100)-2 × 1 surface and 12.9 kcal/mol on the Ge(100)-2 × 1 surface. As a consequence, the branching ratio of the two kinetically competing reactions will be higher on the Ge(100)-2 × 1 surface, especially at low temperatures. Therefore, the Ge(100)-2 × 1 surface is more selective toward the kinetically most stable product when there are multiple kinetically competing reaction pathways. Consequently, a larger fraction of the major product will be formed on the Ge(100)-2 × 1 surface. For example, our calculations suggest that a larger fraction of the hetero-[4 + 2] product will form on

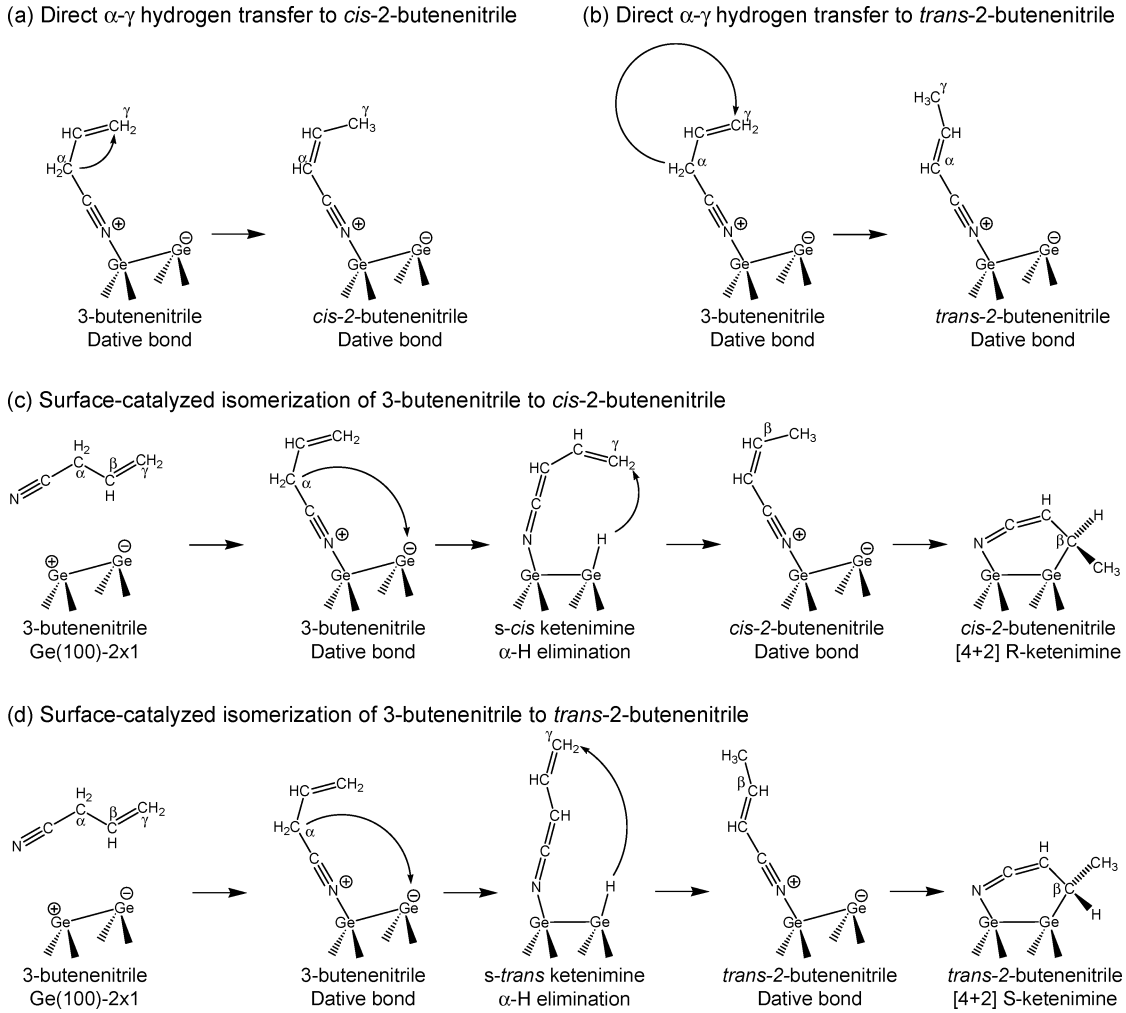

Figure 9. Reaction pathway for the conversion of 3-butenenitrile to 2-butenenitrile on the Ge(100)-2 × 1 surface. (a) Direct α−γ hydrogen transfer of dative-bonded 3-butenenitrile to *cis*-2-butenenitrile; (b) direct α−γ hydrogen transfer of dative-bonded 3-butenenitrile to *trans*-2-butenenitrile; (c) surface-catalyzed isomerization of 3-butenenitrile to *cis*-2-butenenitrile; and (d) surface-catalyzed isomerization of 3-butenenitrile to *trans*-2-butenenitrile.

the Ge(100)-2 × 1 surface than on the Si(100)-2 × 1 surface following reaction of 2-propenenitrile.

We have also investigated the hetero-[4 + 2] reaction of 2-propenenenitrile across two adjacent dimers in a dimer row. An interdimer hetero-[4 + 2] reaction forms a ketenimine in a seven-membered ring, instead of the six-membered ring found in single dimer reactions on the Si(100)-2 × 1 and Ge(100)-2 × 1 surfaces. The longer interdimer distances between adjacent Si−Si (3.84 Å) and Ge−Ge (4.00 Å) dimers compared to the bond lengths of the Si−Si (2.22 Å) and Ge−Ge (2.33 Å) dimers are expected to provide a less strained environment for the formation of ketenimine species (C═C═N). The hetero-[4 + 2] reaction paths of 2-propenenitrile on the $Si_{15}H_{16}$ and $Ge_4Si_{11}H_{16}$ two-dimer clusters are shown in Figure 8. Our calculations predict that the ketenimine products across adjacent dimers are indeed more stable than the products on single dimers. However, the activation barriers for interdimer hetero-[4 + 2] reaction across adjacent dimers are slightly higher than those on single dimers. For example, the single dimer hetero-[4 + 2] reaction of 2-propenenitrile on the Si(100)-2 × 1 surface has an adsorption energy of −37.3 kcal/mol and an activation barrier of 7.8 kcal/mol with respect to the dative-bonded state, while the interdimer hetero-[4 + 2] reaction has an adsorption energy of −40.6 kcal/mol and an activation barrier of 9.1 kcal/mol.

These theoretical results help guide interpretation of the experimental results available for 2-propenenitrile on the Si(100)-2 × 1 and Ge(100)-2 × 1 surfaces. HREELS experiments[5] on the Si(100)-2 × 1 surface indicated that 2-propenenitrile reacts selectively on the surface via C≡N [2 + 2] cycloaddition,[5] whereas MIR-FTIR,[11] PES,[10] and NEXAFS[10] identified the hetero-[4 + 2] product as the major product, along with other side products, on the surface.[10,11] The experimental results suggest that the hetero-[4 + 2] is the major product on the Si(100)-2 × 1 surface, while minor C≡N [2 + 2] and C═C [2 + 2] cycloaddition products are also formed. Our calculations show that the hetero-[4 + 2] reaction has a similar activation barrier (6.9 kcal/mol below the energy of the reactants) to the C≡N [2 + 2] cycloaddition reaction (6.6 kcal/mol below the energy of the reactants), and that the two reactions will compete kinetically on the Si(100)-2 × 1 surface, consistent with the experimental observations.[5,10,11]

A possible explanation for the discrepancy between the HREELS and MIR-FTIR experiments is that HREELS is not sensitive to the ketenimine mode. Due to a dipole scattering mechanism, HREELS probes primarily vibrational modes perpendicular to the surface. The impact scattering mechanism, which can probe modes both parallel and perpendicular to the surface, results in much weaker vibrational features. The hetero-[4 + 2] product consists of a ketenimine (C═C═N) oriented

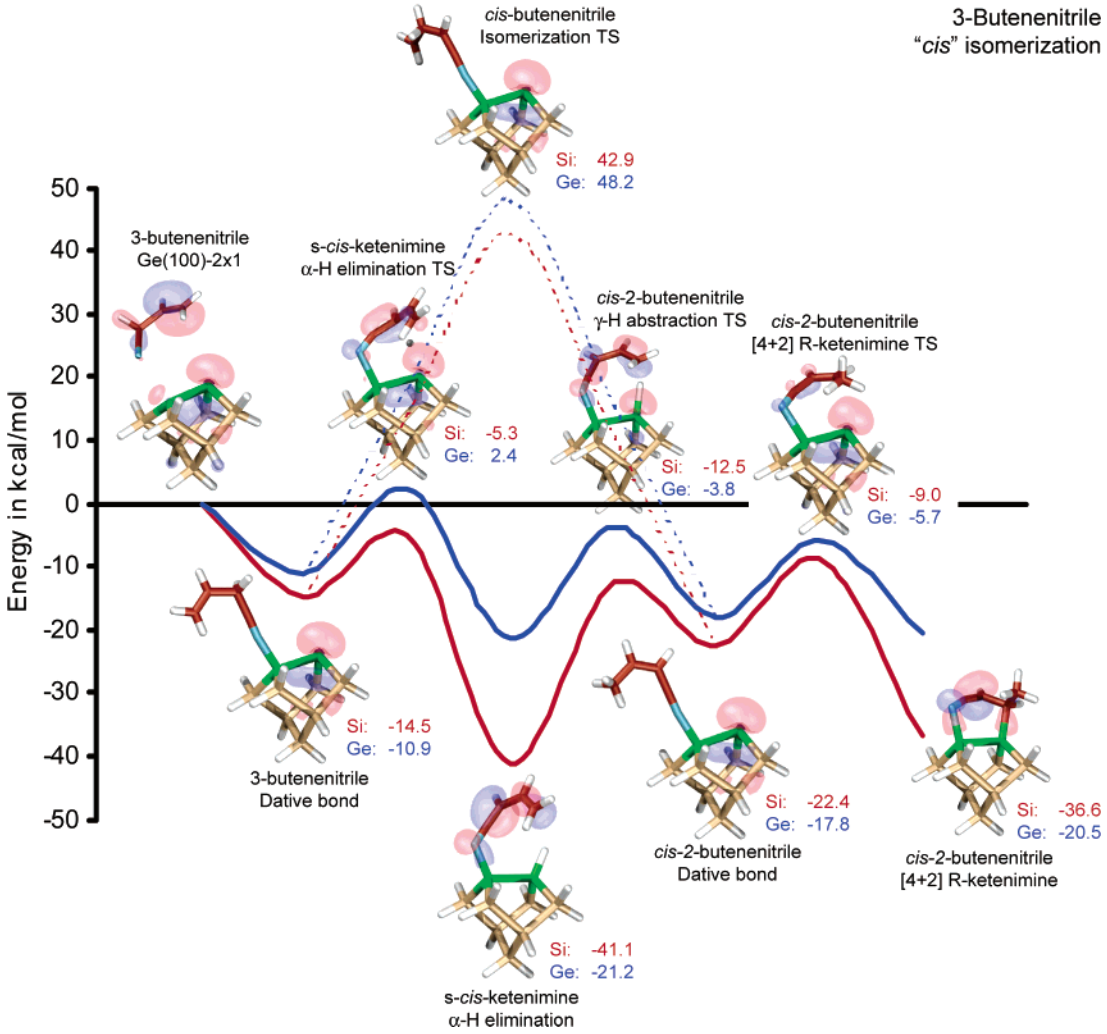

Figure 10. Surface reaction pathway for the isomerization of 3-butenenitrile to *cis*-2-butenenitrile. The red and blue curves depict the reaction paths on the Si(100)-2 × 1 and Ge(100)-2 × 1 surfaces, respectively. Solid lines represent surface-catalyzed pathways, and dotted lines represent direct isomerization between dative-bonded states. Optimized HOMOs on the $Ge_2Si_7H_{12}$ cluster are shown, and the energies are in kcal/mol.

approximately parallel to the surface, as shown in Figure 7a. As a result, the ketenimine asymmetric stretching mode between 1900 and 2100 cm^{-1} would have a dipole moment parallel to the surface, an orientation difficult to probe by HREELS. The HREELS spectrum of 2-propenenitrile on Si(100)-2 × 1 surface at 110 K does possess weak vibrational features at 1930 and 2010 cm^{-1}, which may originate from the ketenimine asymmetric stretch, indicating the presence of the hetero-[4 + 2] reaction product on the surface. Although these HREELS features are weak, they may nonetheless represent a significant amount of hetero-[4 + 2] product on the Si(100)-2 × 1 surface. MIR-FTIR experiments by Schwartz et al.,[11] on the other hand, clearly show that the reaction of 2-propenenitrile on the Si(100)-2 × 1 surface results in the formation of a ketenimine species, consistent with our theoretical predictions.

Our calculations on the $Ge_2Si_7H_{12}$ cluster are consistent with MIR-FTIR experiments on the Ge(100)-2 × 1 surface,[7] which identified the hetero-[4 + 2] adduct as the major product, with a small amount of C═C [2 + 2] product also present. Our calculations also show that the hetero-[4 + 2] reaction is kinetically favored over the C═C [2 + 2] reaction, and hence the ketenimine product resulting from hetero-[4 + 2] reaction of 2-propenenitrile should be the major product on the Ge(100)-2 × 1 surface, as observed experimentally.[7]

3-Butenenitrile. The positions of the C═C and C≡N bonds in 3-butenenitrile (CH_2═CH−CH_2−C≡N) prevent the molecule from undergoing the hetero-[4 + 2] reaction on the Si(100)-2 × 1 and Ge(100)-2 × 1 surfaces. Initial MIR-FTIR experiments indicate, however, that the reaction of 3-butenenitrile results in the formation of ring-ketenimine species on both the Si(100)-2 × 1 and the Ge(100)-2 × 1 surfaces.[7,11] Although the experimental observations can be explained by the isomerization of 3-butenenitrile to 2-butenenitrile, either before or after reaction on the Si(100)-2 × 1 and Ge(100)-2 × 1 surfaces, followed by hetero-[4 + 2] reaction of 2-butenenitrile to form the ring-ketenimine species, subsequent studies suggest that the formation of the ring-ketenimine species can be attributed to contamination of 3-butenenitrile with 2-butenenitrile before reaction on the Ge(100)-2 × 1 surface.[7,11] However, the studies pose an interesting question: can the semiconductor surface catalyze the isomerization reactions? Therefore, we have calculated several isomerization pathways on the Si(100)-2 × 1 and Ge(100)-2 × 1 surfaces in order to explore the possibility of surface-catalyzed isomerization reactions.

Isomerization of 3-butenenitrile to 2-butenenitrile in the gas phase is thermodynamically favorable, due to the greater stability of the conjugated C═C and C≡N bonds in 2-butenenitrile. In particular, *cis*- and *trans*-2-butenenitrile are more stable than 3-butenenitrile by 5.6 and 5.7 kcal/mol, respectively, according to our DFT calculations. However, isomerization of 3-butenenitrile via direct α−γ hydrogen transfer to form either *cis*- or

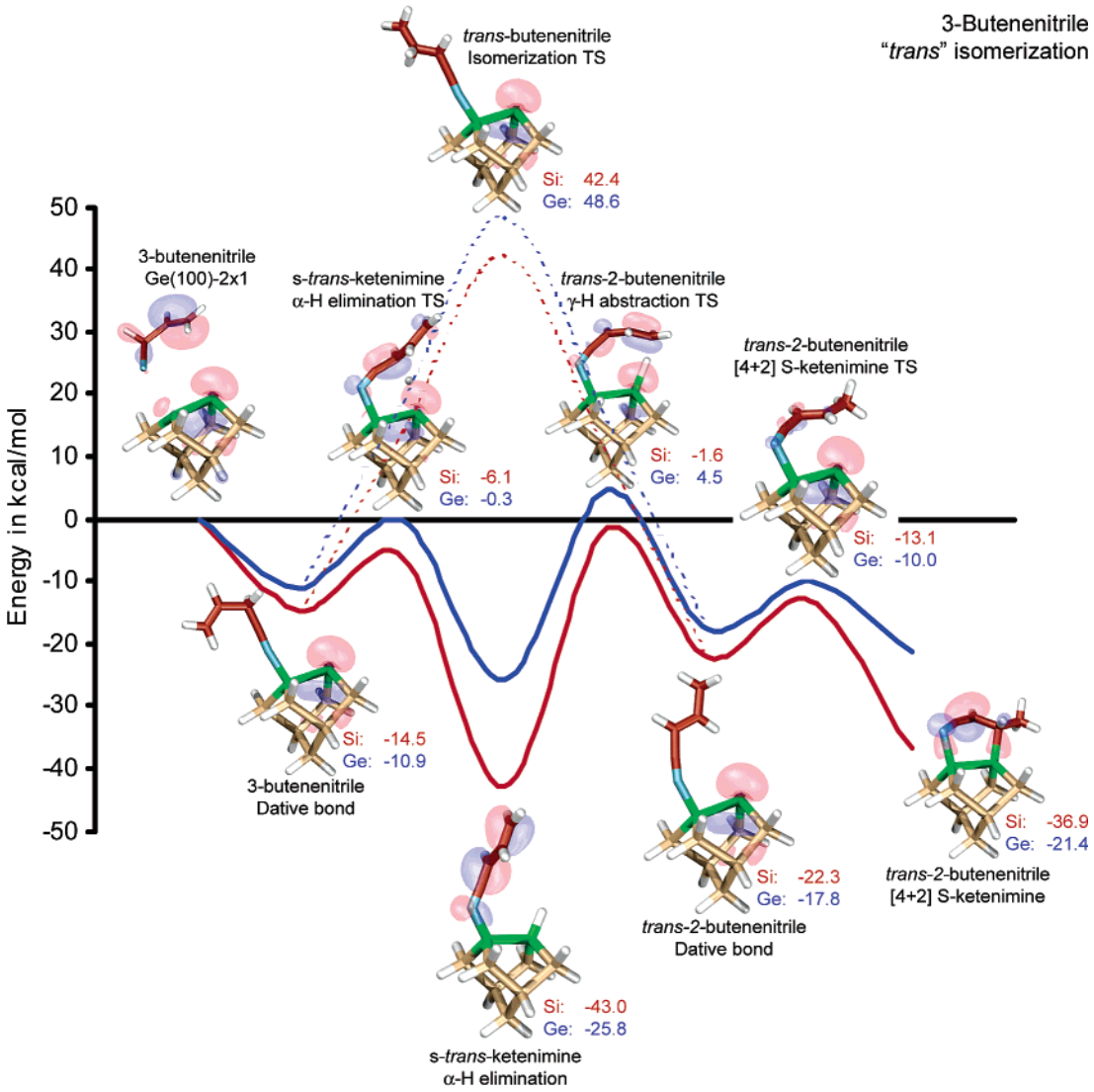

Figure 11. Surface reaction pathway for the isomerization of 3-butenenitrile to *trans*-2-butenenitrile. The red and blue curves depict the reaction paths on the Si(100)-2 × 1 and Ge(100)-2 × 1 surfaces, respectively. Solid lines represent surface-catalyzed pathways, and dotted lines represent direct isomerization between dative-bonded states. Optimized HOMOs on the $Ge_2Si_7H_{12}$ cluster are shown, and the energies are in kcal/mol.

trans-2-butenenitrile in the gas phase has activation barriers of 64.5 and 65.4 kcal/mol, respectively. These barriers are much too high to be overcome thermally at room temperature. Therefore, if ring-ketenimine formation is preceded by conversion of 3-butenenitrile to 2-butenenitrile, the isomerization reaction must be catalyzed in some way, possibly by the Si(100)-2 × 1 or Ge(100)-2 × 1 surfaces.

The simplest isomerization pathways for 3-butenenitrile to 2-butenenitrile involve direct α−γ hydrogen transfer of dative-bonded 3-butenenitrile at the Si(100)-2 × 1 and Ge(100)-2 × 1 surfaces (Figure 9a,b). Energetics and transition states for direct surface-catalyzed isomerization of 3-butenenitrile to *cis*- and *trans*-2-butenenitrile are shown as the dotted pathways of Figure 10 and Figure 11, respectively. For direct α−γ hydrogen transfer from 3-butenenitrile to *cis*-2-butenenitrile, the activation barriers are 57.4 and 59.1 kcal/mol with respect to the dative-bonded state at the Si(100)-2 × 1 and Ge(100)-2 × 1 surfaces, respectively. Activation barriers for direct α−γ hydrogen transfer to form *trans*-2-butenenitrile are 56.9 and 59.5 kcal/mol with respect to dative-bonded 3-butenenitrile at the two surfaces, respectively. These activation barriers for direct α−γ hydrogen transfer from dative-bonded states are reduced compared to conversion in the gas phase. However, direct α−γ hydrogen transfer from dative-bonded states is still highly activated and thus isomerization of 3-butenenitrile is not expected to proceed via direct α−γ hydrogen transfer at either the Si(100)-2 × 1 or Ge(100)-2 × 1 surfaces.

Other isomerization pathways are possible in addition to direct α−γ hydrogen transfer at the dative-bonded 3-butenenitrile state. For example, the isomerization of 3-butenenitrile to 2-butenenitrile in solution is catalyzed in the presence of bases.[24,25] Therefore, it is possible that the nucleophilic dimer atoms on the Si(100)-2 × 1 or Ge(100)-2 × 1 surfaces provide an alternative, low-barrier pathway for the isomerization of 3-butenenitrile to 2-butenenitrile. Some possible surface-catalyzed isomerization pathways for the conversion from 3-butenenitrile to *cis*- and *trans*-2-butenenitrile at the Si(100)-2 × 1 and Ge(100)-2 × 1 surfaces are outlined in Figure 9. The energies of the optimized structures are shown in Figure 10 and Figure 11 for the conversion to *cis*- and *trans*-2-butenenitrile, respectively.

The pathway shown for the conversion of 3-butenenitrile to *cis*-2-butenenitrile (Figure 10) proceeds by α-H elimination of dative-bonded 3-butenenitrile to form a linear, vertical ketenimine in the *s*-cis configuration with an H atom bonded to the surface dimer. This is followed by abstraction of the surface

hydrogen by the γ-carbon of the vertical ketenimine, which leads to dative-bonded 2-butenenitrile in its cis form. Subsequent hetero-[4 + 2] reaction of *cis*-2-butenenitrile on the surface dimer results in the formation of a six-membered ring ketenimine, similar to the hetero-[4 + 2] reaction of 2-propenenitrile. The mechanism proposed for the surface-catalyzed isomerization from 3-butenenitrile to *trans*-2-butenenitrile (Figure 11) has a reaction pathway similar to that for the cis isomer, except that the vertical ketenimine intermediate is in its *s*-trans configuration. The final ring ketenimine products from the cis and trans pathways are identical, except that the β-carbon of the ring ketenimine, which bonds to the surface dimer atom, is chiral. Consequently, the hetero-[4 + 2] reaction of *cis*-2-butenenitrile results in the *R*-enantiomer, while the *S*-enantiomer is formed by the trans isomerization pathway.

The calculations show that although the surface-catalyzed pathways involve more reaction steps, they have lower overall activation barriers than the direct $\alpha-\gamma$ hydrogen transfer pathways. In particular, the activation barriers of the direct $\alpha-\gamma$ hydrogen transfer pathways on the Si(100)-2 × 1 and Ge(100)-2 × 1 surfaces are all above 40 kcal/mol, and therefore the rate of direct $\alpha-\gamma$ hydrogen transfer would be too slow for isomerization to proceed at room temperature. On the other hand, all the surface-catalyzed pathways have overall activation barriers less than 5 kcal/mol with respect to the energy of the reactants, which can be easily surmounted by thermal energy at room temperature. Therefore, the surface-catalyzed pathways are kinetically more favorable than the direct $\alpha-\gamma$ hydrogen transfer pathways for isomerization of 3-butenenitrile.

There are two ketenimine species on the surface-catalyzed isomerization pathways at the Si(100)-2 × 1 and Ge(100)-2 × 1 surfaces. The first one is the vertical ketenimine intermediate resulting from α-H elimination of 3-butenenitrile, and the second one is the final six-membered ring ketenimine product resulting from hetero-[4 + 2] reaction of 2-butenenitrile. The equilibrium distribution of vertical- and ring-ketenimine species can be estimated on the basis of simple thermodynamic analysis. On the Si(100)-2 × 1 surface, the *s*-cis vertical ketenimine is 4.5 kcal/mol more stable than the *R*-ring ketenimine, which means that at equilibrium only 0.53% of the ketenimines are in the *R*-ring form at 300 K. Similarly, due to the 6.1 kcal/mol energy difference between the *s*-trans vertical ketenimine and the *S*-ring ketenimine species on the Si(100)-2 × 1 surface, only 0.004% of the ketenimines are expected to exist is the S-ring form at 300 K at equilibrium. Therefore, complete isomerization of 3-butenenitrile is not likely to occur on the Si(100)-2 × 1 surface, and the N═C═C vibrational mode observed on the surface is also unlikely to originate from complete isomerization of 3-butenenitrile.

According to the DFT calculations, the energy differences between the vertical and ring ketenimines on the Ge(100)-2 × 1 surface are 0.7 and 4.3 kcal/mol for the cis and trans pathways, respectively. Using a simple thermodynamic analysis, the equilibrium coverages of *R*- and *S*-ring ketenimines are calculated to be 30.9% and 0.07% at 300 K, respectively. Although a significant amount of *R*-ring ketenimine is predicted to form on the Ge(100)-2 × 1 surface, the observed ring ketenimine species were not attributed to surface-catalyzed isomerization of 3-butenenitrile.[7] Since the observed distribution does not match the equilibrium thermodynamics predictions, we explore the role of kinetics on the final product distribution. We have simulated the time-dependent coverage of each surface species on the Ge(100)-2 × 1 surface and quantified the amount of ring ketenimine species formed from surface-catalyzed isomerization. Specifically, we have incorporated the kinetic parameters determined by DFT into a kinetic model of the surface-catalyzed isomerization process. A set of ordinary differential rate equations, shown below in the group of equations labeled (1), is solved to determine the coverage of each surface species, which include dative-bonded 3-butenenitrile (A), *s*-cis and *s*-trans vertical ketenimines (B_{ci} and B_{tr}), dative-bonded *cis*- and *trans*-2-butenenitriles (C_{ci} and C_{tr}), and *R*- and *S*-ring ketenimine species (D_{ci} and D_{tr}). The rate constants in the kinetic model are calculated from the activation barriers determined by DFT at 300 K, and the preexponential factors are calculated by canonical transition state theory using the frequencies calculated by B3LYP-DFT. In eq 1, subscripts A, B, C, and D denote the species, and ci and tr denote cis and trans isomers, respectively. Superscripts "for", "rev", and "des" denote forward, reverse, and desorption rates, respectively. The fast conversion between *s*-cis and *s*-trans vertical ketenimines is also included in the kinetic model, the rate constants of which are denoted by k^{ct}_{BB} and k^{tc}_{BB}.

$$\frac{dA(t)}{dt} = -k^{des}_{A}A(t) - k^{for}_{AB,tr}A(t) - k^{for}_{AB,ci}A(t) + k^{rev}_{AB,tr}B_{tr}(t) + k^{rev}_{AB,ci}B_{ci}(t)$$

$$\frac{dB_{ci}(t)}{dt} = k^{for}_{AB,ci}A(t) - k^{rev}_{AB,ci}B_{ci}(t) - k^{for}_{BC,ci}B_{ci}(t) + k^{rev}_{BC,ci}C_{ci}(t) - k^{ct}_{BB}B_{ci}(t) + k^{tc}_{BB}B_{tr}(t)$$

$$\frac{dB_{tr}(t)}{dt} = k^{for}_{AB,tr}A(t) - B_{tr}(t) - k^{for}_{BC,tr}B_{tr}(t) + k^{rev}_{BC,tr}C_{tr}(t) - k^{tc}_{BB}B_{tr}(t) + k^{ct}_{BB}B_{ci}(t)$$

$$\frac{dC_{ci}(t)}{dt} = k^{for}_{BC,ci}B_{ci}(t) - k^{rev}_{BC,ci}C_{ci}(t) - k^{for}_{CD,ci}C_{ci}(t) + k^{rev}_{CD,ci}D_{ci}(t) - k^{des}_{C,ci}C_{ci}(t)$$

$$\frac{dC_{tr}(t)}{dt} = k^{for}_{BC,tr}B_{tr}(t) - k^{rev}_{BC,tr}C_{tr}(t) - k^{for}_{CD,tr}C_{tr}(t) + k^{rev}_{CD,tr}D_{tr}(t) - k^{des}_{C,tr}C_{tr}(t)$$

$$\frac{dD_{ci}(t)}{dt} = k^{for}_{CD,ci}C_{ci}(t) - k^{rev}_{CD,ci}D_{ci}(t)$$

$$\frac{dD_{tr}(t)}{dt} = k^{for}_{CD,tr}C_{tr}(t) - k^{rev}_{CD,tr}D_{tr}(t) \quad (1)$$

The time-dependent coverages of the *R*- and *S*-ring ketenimine species on the Ge(100)-2 × 1 surface determined from the kinetic model are shown in Figure 12. The kinetic analysis shows that the coverage of the ketenimine species increases to a pseudo-steady-state concentration within short time scales due to surface-catalyzed isomerization, then decays exponentially at long time scales due to reversible desorption of the ring ketenimine species. As seen from Figure 12, although the surface-catalyzed isomerization reaction pathways have low overall activation barriers, the amount of ring ketenimine formed on the Ge(100)-2 × 1 surface is very small at all time scales (even at early times). The maximum coverage of the *R*-ring ketenimine species on the Ge(100)-2 × 1 surface is predicted to be below 2×10^{-6}, and the amount of *S*-ring ketenimine is below 5×10^{-12}. These surface concentrations are probably under the detection limit of most surface spectroscopic tech-

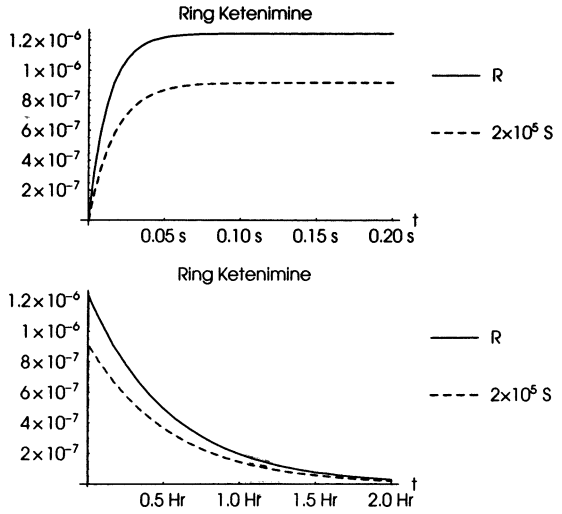

Figure 12. Calculated coverage of *R*- and *S*-ring ketenimine resulting from complete isomerization of 3-butenenitrile on the Ge(100)-2 × 1 surface. The solid lines represent the coverage of *R*-ring ketenimine from the cis pathway and the dotted lines depict the coverage of the *S*-isomer from the trans pathway. Note that the coverages of both ring ketenimines are very low. The coverages of ring ketenimines increase rapidly to their pseudo-steady-state concentrations in short time scales (top), then decay exponentially in long time scales (bottom).

niques. Therefore, according to our calculations, the N═C═C asymmetric stretching mode observed on the Ge(100)-2 × 1 surface is unlikely to originate from surface-catalyzed isomerization of 3-butenenitrile. On the Si(100)-2 × 1 surface, the ring ketenimine species are energetically and kinetically unstable with respect to the vertical ketenimine species.

Although the kinetic analysis shows that complete isomerization of 3-butenenitrile is not likely to occur on semiconductor surfaces, the possibility of surface-catalyzed isomerization opens up new chemical strategies which can be used for the controlled attachment of organic functional groups onto semiconductor surfaces. Specifically, if the ring ketenimine species is energetically more stable, the isomerization process could go to completion and a significant amount of ring ketenimine formed from surface-catalyzed isomerization would be observed on the Si(100)-2 × 1 and Ge(100)-2 × 1 surfaces. This idea of surface-catalyzed isomerization could be used to form stable six-membered ring structures from nonconjugated organic compounds.

Conclusion

We have used density functional theory with cluster models to investigate the chemistry of nitrile compounds on the Si(100)-2 × 1 and Ge(100)-2 × 1 surfaces. Three organic nitrile compounds, namely, acetonitrile ($CH_3-C\equiv N$), 2-propenenitrile ($CH_2=CH-C\equiv N$), and 3-butenenitrile ($CH_2=CH-CH_2-C\equiv N$) are studied. For acetonitrile, our calculations predict that the C≡N [2 + 2] cycloaddition reaction is slightly more favorable kinetically than the α-H elimination reaction on the Si(100)-2 × 1 surface, leading to selective C≡N [2 + 2] reaction at 110 K and a mixture of products at 300 K. However, acetonitrile is not expected to react with the Ge(100)-2 × 1 surface at 300 K, due to fast reversible desorption of either the C≡N [2 + 2] or α-H elimination reaction products. Our calculations show that 3-propenenitrile can react with the Si(100)-2 × 1 and Ge(100)-2 × 1 surfaces through a variety of reaction pathways, including hetero-[4 + 2], C≡N [2 + 2], α-H elimination, and C═C [2 + 2] reactions. In particular, the calculations predict that kinetic competition of multiple reaction pathways should result in a mixture of products for the reaction of 2-propenenitrile on the Si(100)-2 × 1 surface. On the Ge(100)-2 × 1 surface, due to the low kinetic stability of the C≡N [2 + 2] and α-H elimination products, the hetero-[4 + 2] ring ketenimine is predicted to be the major reaction product. Interdimer hetero-[4 + 2] reactions of 2-propenenitrile across two adjacent dimers along a dimer row are also investigated and found to have energetics similar to those on a single dimer.

Motivated by recent experimental observations, we have also studied the possibility of surface-catalyzed isomerization of nonconjugated nitriles. A proposed isomerization mechanism involving consecutive α-H elimination and γ-H abstraction of 3-butenenitrile catalyzed by the Si(100)-2 × 1 and Ge(100)-2 × 1 surfaces was examined. Our calculations show that complete isomerization of 3-butenenitrile to 2-butenenitrile can proceed without significant overall activation barriers on both surfaces by this pathway. Isomerization pathways for the conversion to *cis*- and *trans*-2-butenenitrile, which subsequently lead to chiral ring keteminines on the two surfaces, are calculated. Although kinetic analysis predicts only negligibly small amounts of ring keteminines formed on the Ge(100)-2 × 1 surface, the idea of surface-catalyzed isomerization can be applied to other organic functionalities to form stable ring structures from nonconjugated organic compounds.

Acknowledgment. The authors thank George T. Wang for insightful discussions. M.A.F. acknowledges the National Science Foundation for financial support in the form of a Graduate Research Fellowship. S.F.B. acknowledges financial support from the National Science Foundation (CHE 9900041 and CHE 0245260) and the Stanford University Center for Integrated Systems. S.F.B. is a Camille Dreyfus Teacher-Scholar. C.B.M. thanks the Charles Powell Foundation for funding. This work was partially supported by the National Computational Science Alliance.

References and Notes

(1) Wolkow, R. A. *Annu. Rev. Phys. Chem.* **1999**, *50*, 413−441.
(2) Hamers, R. J.; Coulter, S. K.; Ellison, M. D.; Hovis, J. S.; Padowitz, D. F.; Schwartz, M. P.; Greenlief, C. M.; Russell, J. N. *Acc. Chem. Res.* **2000**, *33*, 617−624.
(3) Bent, S. F. *J. Phys. Chem. B* **2002**, *106*, 2830−2842.
(4) Buriak, J. M. *Chem. Rev.* **2002**, *102*, 1271−1308.
(5) Tao, F.; Sim, W. S.; Xu, G. Q.; Qiao, M. H. *J. Am. Chem. Soc.* **2001**, *123*, 9397−9403.
(6) Tao, F.; Wang, Z. H.; Qiao, M. H.; Liu, Q.; Sim, W. S.; Xu, G. Q. *J. Chem. Phys.* **2001**, *115*, 8563−8569.
(7) Filler, M. A.; Mui, C.; Musgrave, C. B.; Bent, S. F. *J. Am. Chem. Soc.* **2003**, *125*, 4928−4936.
(8) Lu, X.; Lin, M. C. *Int. Rev. Phys. Chem.* **2002**, *21*, 137−184.
(9) Lu, X.; Xu, X.; Wu, J. M.; Wang, N. Q.; Zhang, Q. *New J. Chem.* **2002**, *26*, 160−164.
(10) Bournel, F.; Gallet, J.; Kubsky, S.; Dufour, G.; Rochet, F.; Simeoni, M.; Sirotti, F. *Surf. Sci.* **2002**, *513*, 37−48.
(11) Schwartz, M. P.; Hamers, R. J. *Surf. Sci.* **2002**, *515*, 75−86.
(12) Choi, C. H.; Gordon, M. S. *J. Am. Chem. Soc.* **2002**, *124*, 6162−6167.
(13) Hohenberg, P.; Kohn, W. *Phys. Rev.* **1964**, *136*, B864−B871.
(14) Kohn, W.; Sham, L. J. *Phys. Rev.* **1965**, *140*, A1133−A1138.
(15) Konecny, R.; Doren, D. J. *Surf. Sci.* **1998**, *417*, 169−188.
(16) Wang, G. T.; Mui, C.; Musgrave, C. B.; Bent, S. F. *J. Am. Chem. Soc.* **2002**, *124*, 8990−9004.
(17) Lee, C. T.; Yang, W. T.; Parr, R. G. *Phys. Rev. B* **1988**, *37*, 785−789.
(18) Becke, A. D. *J. Chem. Phys.* **1993**, *98*, 5648−5652.
(19) Frisch, M. J.; Trucks, G. W.; Schlegel, H. B.; Scuseria, G. E.; Robb, M. A.; Cheeseman, J. R.; Zakrzewski, V. G.; Montgomery, J. A., Jr.; Stratmann, R. E.; Burant, J. C.; Dapprich, S.; Millam, J. M.; Daniels, A. D.; Kudin, K. N.; Strain, M. C.; Farkas, O.; Tomasi, J.; Barone, V.; Cossi, M.; Cammi, R.; Mennucci, B.; Pomelli, C.; Adamo, C.; Clifford, S.; Ochterski, J.; Petersson, G. A.; Ayala, P. Y.; Cui, Q.; Morokuma, K.; Rega,

N.; Salvador, P.; Dannenberg, J. J.; Malick, D. K.; Rabuck, A. D.; Raghavachari, K.; Foresman, J. B.; Cioslowski, J.; Ortiz, J. V.; Baboul, A. G.; Stefanov, B. B.; Liu, G.; Liashenko, A.; Piskorz, P.; Komaromi, I.; Gomperts, R.; Martin, R. L.; Fox, D. J.; Keith, T.; Al-Laham, M. A.; Peng, C. Y.; Nanayakkara, A.; Challacombe, M.; Gill, P. M. W.; Johnson, B.; Chen, W.; Wong, M. W.; Andres, J. L.; Gonzalez, C.; Head-Gordon, M.; Replogle, E. S.; Pople, J. A. *Gaussian 98;* Gaussian, Inc.: Pittsburgh, PA, 2001.

(20) Baetzold, R. C.; Somorjai, G. A. *J. Catal.* **1976**, *45*, 94−105.

(21) Mui, C.; Han, J. H.; Wang, G. T.; Musgrave, C. B.; Bent, S. F. *J. Am. Chem. Soc.* **2002**, *124*, 4027−4038.

(22) Wang, G. T.; Mui, C.; Musgrave, C. B.; Bent, S. F. *J. Phys. Chem. B* **2001**, *105*, 12559−12565.

(23) Bent, H. A. *Chem. Rev.* **1961**, *61*, 275−311.

(24) Bordwell, F. G.; Hughes, D. L. *J. Org. Chem.* **1983**, *48*, 619−621.

(25) Bordwell, F. G.; Hughes, D. L. *J. Am. Chem. Soc.* **1985**, *107*, 4737−4744.